Scilight

Review

Advancements in Luminescent Metal-Organic Cages: Applications and Future Prospects

Osama Younis [1,2,*], Xiangyun Xiao [1], Jianxun Yang [3], Kamal I. Aly [4], Etify A. Bakhite [4], and Xinchun Yang [1,*]

[1] Institute of Technology for Carbon Neutrality, Shenzhen Institute of Advanced Technology (SIAT), Chinese Academy of Sciences (CAS), Shenzhen 518055, China
[2] Chemistry Department, Faculty of Science, New Valley University, El-Kharga 72511, Egypt
[3] Three Gorges Daofu Renewables Co., Ltd. Ganzi 626700, China
[4] Chemistry Department, Faculty of Science, Assiut University, Asyut 71516, Egypt
* Correspondence: osamayounis@sci.nvu.edu.eg (O.Y.); xc.yang@siat.ac.cn or yang.xinchun@hotmail.com (X.Y.)

Abstract: Researchers worldwide are developing innovative luminescent systems with exceptional features like high sensitivity. Luminescent frameworks based on aggregation-induced emission (AIE) have emerged as promising candidates for various applications. Over the past decade, porous materials like metal-organic cages (MOCs) incorporating AIE luminogens (AIEgens) have demonstrated exceptional performance. Chirality plays a significant role in specific non-racemic luminescent systems, particularly circularly polarized luminescence (CPL). Chiral organic materials coordinated with metals, including MOCs, have gained importance as they combine organic ligands and coordination-bonded metal centers, enabling the design of novel structures with CPL. These materials have shown exciting potential applications in fields like CPL-OLED, chiral recognition, and sensing. This review article provides an overview of the recent progress in emissive porous materials, specifically MOCs, and their possible applications. Additionally, the review focuses on the recent progress in AIE$_{gen}$-based cages, CPL-active cages, and non-AIE$_{gen}$-based cages, their practical applications in sensing and enantioselectivity, and future prospects. Key challenges in AIE-based POCs and MOCs include limited stability, affecting their use in wide-surface thin films, and the need to understand molecular structure and topology impacts. Future efforts should enhance luminescence efficiency and explore applications in chiral sensing, supramolecular assemblies, bioimaging, and optoelectronics, driving innovation in smart materials.

Keywords: uminescence; metal-organic cages; porous; AIE luminogens; sensing; enantioselectivity

1. Introduction

The global scientific community is increasingly interested in luminescent materials due to their remarkable sensing capabilities, higher energy conversion efficiency, improved resolution, and in-situ operation [1–5]. These materials have shown great potential in various practical applications, particularly in the fields of sensors, guest probes, bio-imaging, light-emitting devices, and organic electrical devices. However, a common issue faced by conventional fluorescent dyes is the phenomenon known as aggregation-caused quenching (ACQ), which originates a decrease or complete loss of emission upon molecular aggregation [6]. This ACQ effect severely limits the luminous efficiency of most luminescent materials in the solid state, hindering their applications. Notably, the finding of the aggregation-induced emission (AIE) phenomenon has revolutionized the design of light-emitting materials and has generated significant interest across different scientific disciplines, including chemistry, physics, materials science, and life science [6,7]. AIE luminogens (AIE$_{gens}$) possess exclusive properties such as high photostability and extraordinary quantum yield, making them highly desirable for multiple applications, including theranostics, antibacterial agents, OLEDs, bioimaging, and stimulus-responsive detection [8–14].

Metal-organic cages (MOCs), a new class of luminescent materials, are discrete coordination assemblies with well-defined structures, symmetrical topologies, distinct architectures, internal cavities, and the ability to non-covalently enclose guest molecules [15–19]. MOCs are versatile materials with a wide range of applications. They are effective in gas storage and separation, enabling selective adsorption of gases like hydrogen and carbon dioxide. MOCs serve as catalysts, drug delivery systems, and sensors due to their tunable structures and high surface area. Their luminescent properties make them suitable for bioimaging and optoelectronic devices, while their ability to non-

adsorb pollutants supports environmental remediation efforts. Additionally, MOCs can facilitate chiral recognition and separation in pharmaceutical chemistry, highlighting their potential across various fields, including materials science and biomedical applications. Numerous self-assembled cages made of metal-organic compounds have been successfully synthesized, capable of hosting multiple guests through specific host-guest interactions and nonspecific supramolecular interrelations like van der Waals forces, Coulombic interactions, hydrogen bonding, and steric interactions. In addition, the combined influence of geometry, solvation, and dielectric behavior strengthens the affinity for guest molecules within the host cages [15]. Metal centers serve as vertices during the construction of MOCs, while organic ligands act as faces or edges depending on their binding numbers and positions [20]. When AIE$_{gens}$ are incorporated into porous materials like MOCs, several exclusive advantages are observed. For instance, energy bandgap, emission color, wavelength atomic arrangement, and packing mode can be easily modified by incorporating metal nodes and organic ligands. The inherent rigidity of AIE$_{gens}$, resulting from their rigid molecular structures, effectively suppresses intramolecular motion, thereby avoiding self-quenching and suggestively enhancing emission behavior. Finally, AIE-based MOCs and other porous organic cages (POCs) exhibit highly controllable pore sizes and a porous architecture that enables precise control of the inner chemical environment. These activities facilitate specific and strong interactions between guest molecules and the AIE$_{gen}$ integrated within the frameworks, thus significantly enhancing the potential application effectiveness of the AIE$_{gen}$-based frameworks [15]. In addition, non-AIE$_{gen}$ luminogens can also be utilized to build up porous AIE-based molecules with efficient photoluminescence [21,22].

Circularly polarized luminescence (CPL) is a fascinating optical phenomenon where light is emitted with a preferred circular polarization in chiral luminescent systems [23,24]. Recently, there has been significant interest in CPL materials due to their potential for advanced applications such as smart sensors, optoelectronics, photonics, optical information storage and security, chiral catalysis, chiral recognition, biological imaging and diagnostics, and 3D displaying [25–30]. However, a major challenge in utilizing CPL for 3D optical storage and imaging is the difficulty of preparing chiral compounds that exhibit both strong emission and a high dissymmetry factor (g_{lum}) [31]. One possible approach to address this challenge is introducing chiral groups into pre-assembled POCs, which can emerge new features. For instance, the optical properties of metal-coordinated chiral cages can be tuned through ligand adjustment or by incorporating specific guest molecules [32]. Although post-assembly modification on regulating the chirality of POCs has the potential to expand their applications, it has not been effectively developed due to the restricted stability and solubility of many POCs in solvents, which limits their exploration in the field of chirality [33,34]. Post-assembly modification provides a method for precisely controlling the solubility and host–guest characteristics of an imine-based cage [35]. Additionally, a chiral MOC was integrated into a porous framework using this approach, which facilitated the examination of its host-guest chemistry in the solid state through single-crystal diffraction techniques [36]. Moreover, a novel phosphine-paneled supramolecular cage framework was developed, allowing for rational modification of its anion binding capabilities via selective post-assembly functionalization [37].

Even though MOCs offer great potential in applications such as gas storage, catalysis, and drug delivery, their practical use in industry faces significant challenges, particularly regarding stability, cost of synthesis, and industrial scalability. One of the primary concerns is the stability of MOCs under operational conditions. Many MOCs suffer from poor chemical stability, especially in humid environments or aqueous media, due to the vulnerability of their metal-ligand bonds to hydrolysis [38]. Additionally, their thermal stability is often lower compared to other porous materials like zeolites, making them unsuitable for high-temperature processes commonly used in industrial settings [39]. The mechanical fragility of MOCs, stemming from their crystalline structures, further limits their capacity to withstand the stresses of large-scale manufacturing and transportation. Another critical issue is the cost of synthesis [40]. MOCs typically require complex, energy-intensive processes and expensive organic ligands, which hinder their scalability. The high purity of metal ions and organic ligands needed, combined with low yields, makes scaling up the production of MOCs economically challenging. Furthermore, many MOCs need post-synthetic modifications to enhance their stability or functionality, which adds additional cost and complexity. From an industrial application standpoint, MOCs present challenges related to their processability and reuse. Fabricating MOCs into usable forms, such as membranes or films, is difficult due to their mechanical weakness [41]. This limits their integration into existing industrial systems. Additionally, their performance often degrades after repeated use cycles, particularly in catalytic or gas storage applications, where they must maintain functionality over long periods. Developing more robust metal-ligand interactions, designing covalent organic cages, and hybridizing MOCs with other materials are potential solutions being explored to enhance their stability and make them more suitable for industrial applications. Addressing these challenges requires innovative approaches to reduce synthesis costs, improve the processability of MOCs, and develop methods to increase their durability in real-world conditions. Collaboration across chemistry, materials science,

and engineering is essential to overcome the current limitations and unlock the full potential of MOCs for industrial-scale applications.

This review aims to offer a resource for researchers, consolidating the progress on luminescent MOCs and POCs. We focus here on various aspects such as AIE$_{gen}$-functionalization, non-AIE$_{gen}$ cages, CPL-active cages, and potential applications with a future-oriented perspective.

2. AIE$_{gen}$-Based Organic Cages

A practical and concise strategy has been developed to create fluorescent organic cages by reducing preorganized metallacages (Figure 1a) [42]. Cage C1 and C2 exhibit strong emissions in the aggregated state due to their AIE features, despite the precursor metallacages being non-fluorescent in both solution and solid states. New tri-Schiff bases (TSBs) based on salicylaldehyde were developed, featuring a non-conjugated trimethylamine bridge (Figure 1b) [43]. These TSBs exhibit strong blue, green, and yellow AIE emission, featuring substantial Stokes shifts (up to 167 nm) and impressive emission quantum yields (up to 0.18). TSB solids demonstrate enantiomeric properties and enhanced mechanochromic fluorescence. These tripod-like and flexible cages effectively host anions, enabling turn-on fluorescence detection. Despite the absence of a conjugated bridge, robust non-covalent interactions effectively restrict intramolecular rotations, leading to pronounced AIE properties. These TSBs have potential as versatile anion hosts and probes. Also, a sulfonation reaction produced an organic cage D-RCC1, exhibiting strong emission with a quantum yield of 42% in dilute organic solution [44]. Remarkably, D-RCC1 exhibited an exceptionally high quantum yield of 92% when aggregated in the solid state (Figure 1c). The symmetrical three-dimensional structure of D-RCC1, with evenly distributed dye molecules successfully prevents interactions among the dyes and ensures robust emission in both aggregated states and individual molecule. Furthermore, a conformation-locking strategy enables the design of MOCs and POCS with luminescence and photochromism in both the solid state and solution (Figure 1d) [45]. FT-RC is a TPE-based cage, and its scaffold restricts the conformation of AIE$_{gens}$, promoting intramolecular photocyclization for photochromism. The rigid scaffold also maintains AIE$_{gen}$ emission in dilute solutions, expanding their applications beyond the solid state.
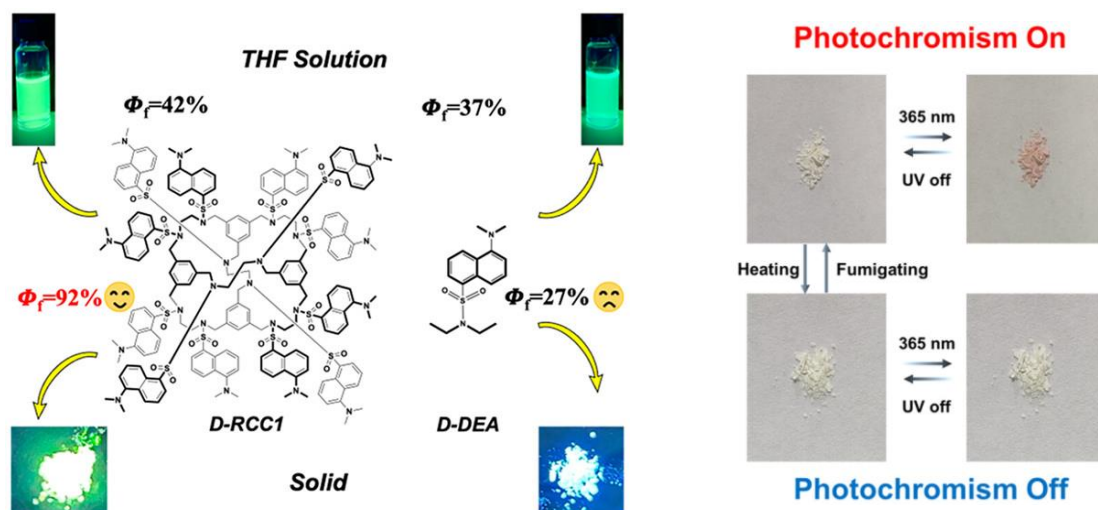
(**a**)

(**b**)

(**c**)

(**d**)
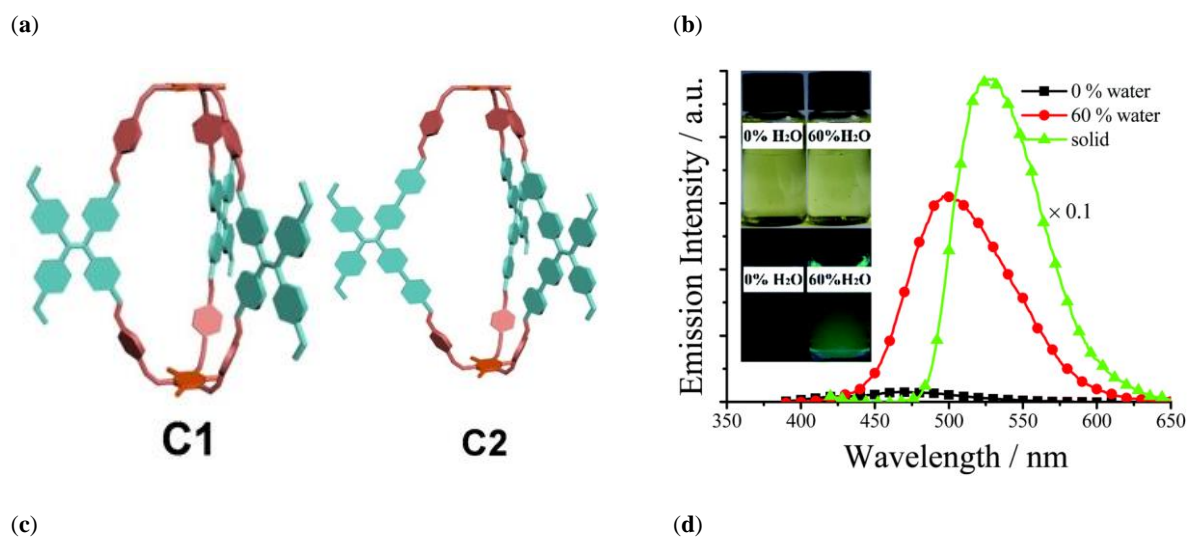
Figure 1. (**a**) Representation of the POCs C1 and C2. Adapted with permission from ref. [42] Copyright © 2023 Wiley-VCH GmbH, John Wiley and Sons. (**b**) AIE behavior of a tri-Schiff base (TSB). Adapted with permission from ref. [43] Copyright © 2023 The Royal Society of Chemistry. (**c**) Intense emission of the cage D-RCC1 both in the solid state and solution. Adapted with permission from ref. [44] Copyright © 2022 American Chemical Society. (**d**) Photochromism of the cage FT-RC. Adapted with permission from ref. [44] Copyright © 2023 American Chemical Society.

Effect of the Solvent and Structural Rigidity

Metallacages offer a platform for systematically exploring their photophysical characteristics due to their structural diversity and adjustability. Various factors, including pressure, temperature, solvents, counterions, and structural rigidity, affect the emission behavior of AIE-active cages [46]. Here, we will focus on the solvent and structural rigidity effect. The solubility of a solvent is crucial in determining the light-emitting behavior of AIE metallacages. Poor solvents generally lead to metallacage aggregation, which can be observed by microscopic techniques [47,48]. For example, increasing the hexane content in Cage-2m resulted in higher average intensity due to changes in morphology, leading to a more compact packing structure that restricted conformational changes of the TPE moieties compared to discrete rigid cages. This caused a blue shift in the emitted light and increased the emission intensity (Figure 2a) [47]. A similar enhancement was observed for other metallacages [49]. The fluorescence of these cages was further enhanced by systematically increasing the proportion of hexane in CH_2Cl_2 solutions by suppressing intramolecular motions of the TPE units following solvent-induced aggregation. Different conformations of AIE metallacages in various solvents and their hydrophobic nature can alter the conjugation degree of TPE units, resulting in changes in emission intensity and wavelength, for example, Cage-1a in Figure 2b [50]. Solvent polarity significantly affects the emission behavior of AIE-active cages by influencing energy transfer processes, including charge transfer between metal centers and AIE_{gens}. Cage-2r exhibited irregular variations in emission intensity and wavelength across different solvents, ranging from nonpolar CCl_4 to highly polar solvents such as water and MeOH (Figure 2c) [47]. Metallacage Cage-2r exhibits different photophysical behavior depending on solubility in a particular solvent. Solvent polarity becomes the main factor influencing light emission when solubility is comparable across solvents. This is due to the effect of solvent polarity on metal-to-ligand charge-transfer (MLCT) processes within the metallacages. Higher solvent polarity enhances MLCT processes but reduces fluorescence efficiency. Modifying the components of metallacages can alter their fluorescence characteristics in response to solvents with varying polarities. Cage-4a to Cage-4c demonstrated pronounced fluorescence in polar aprotic solvents such as acetonitrile, DMSO, and DMF while displaying moderate fluorescence in less polar aprotic solvents like $CHCl_3$, CH_2Cl_2, and acetone, as well as in a polar protic solvent like MeOH, Figure 2d [51]. Despite the variations in fluorescence and underlying mechanisms, it was confirmed that the solvent can efficiently adjust the fluorescence characteristics of TPE-based cages. Structural rigidity is a crucial internal factor influencing the emission behavior of AIE-active metallacages [52]. For example, introducing an extra alkyne group into a metallacage, resulting in increased ligand rigidity, led to a notable enhancement in fluorescence intensity [53].
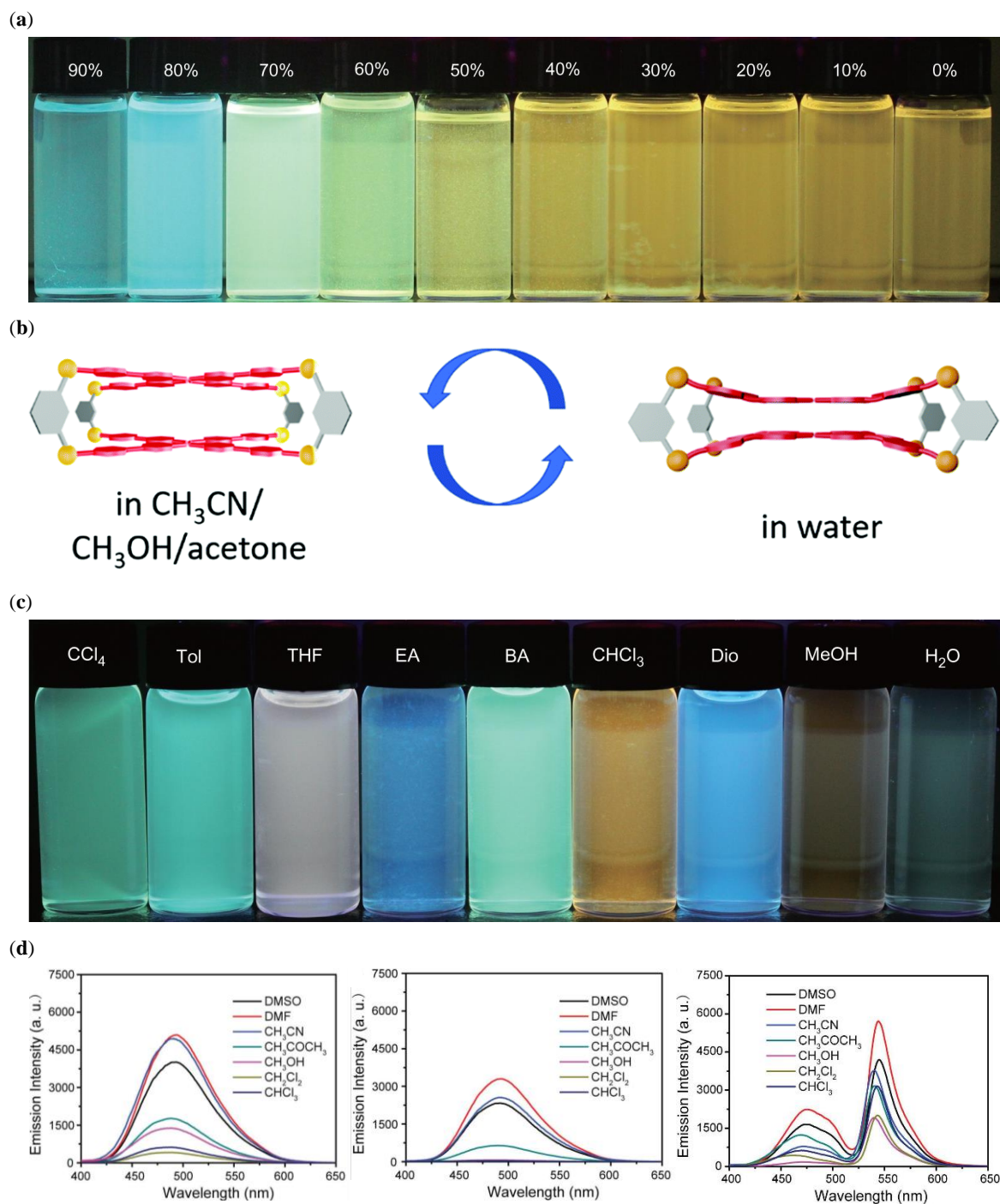
(**a**)

(**b**)

in CH$_3$CN/
CH$_3$OH/acetone

in water

(**c**)

(**d**)

Figure 2. (**a**) Photographs of Cage-2m under excitation at 365 nm in CH$_2$Cl$_2$/hexane mixtures with different hexane fractions. Adapted with permission from ref. [47] Copyright © 2015 Springer Nature. (**b**) Depiction of the hypothesized conformational alteration of Cage-1a in varying solvent environments. Adapted with permission from ref. [50] Copyright © 2019 The Royal Society of Chemistry. (**c**) Photographs of metallacages Cage-2r in different solvents (λ_{ex} = 355 nm). Adapted with permission from ref. [47] Copyright © 2015 Springer Nature. (**d**) Photoluminescence spectra of Cage-4a to Cage-4c (from left to right) in various solvents (λ_{ex} = 365 nm). Adapted with permission from ref. [51] Copyright © 2017 American Chemical Society.

3. Non-AIE$_{gen}$-Based Luminescent Cages

Non-AIE$_{gen}$-based luminescent cages are an emerging area of research that offers unique opportunities for developing luminescent materials. Instead of relying on the AIE effect, these cages utilize other mechanisms to achieve luminescence. By understanding their design principles, optimizing luminescence mechanisms, and exploring their applications and stability, researchers can harness the potential of these cages for a wide range of technological applications. Non-AIEgen-based luminescent cages represent a fascinating category of materials

that exhibit luminescence through mechanisms distinct from AIE. These cages can be constructed from a variety of organic and inorganic components, which allows for significant versatility in their design and application. Commonly, they include metal-organic frameworks (MOFs), coordination polymers, and organic frameworks, each employing a range of ligands and metal centers to achieve specific photophysical properties tailored for diverse uses. One of the key advantages of non-AIEgen-based luminescent cages is their tunability. Researchers can modify the structural elements of these cages, such as the choice of ligands and the types of metal ions used, to precisely control the emission wavelengths and intensities. This ability to tailor luminescent properties makes these cages suitable for a variety of applications, from basic research to advanced technological uses. In addition to their tunable emissions, non-AIEgen-based luminescent cages excel in host-guest chemistry. These cages can encapsulate a wide range of guest molecules, which allows them to serve as platforms for selective sensing, catalysis, and drug delivery. The luminescence of the cages often acts as a sensitive readout for binding events, enabling real-time monitoring of interactions between the cage and its guests. This characteristic is particularly useful in biosensing applications, where detecting specific biomolecules can be crucial for diagnostics and environmental monitoring. Furthermore, the potential applications of non-AIEgen-based luminescent cages extend into fields such as bioimaging, where they can serve as contrast agents, and optoelectronics, where their luminescent properties can be harnessed for light-emitting devices. Their unique structural characteristics and functionality also make them promising candidates for developing advanced materials in nanotechnology and materials science. Overall, non-AIEgen-based luminescent cages offer exciting opportunities for innovation across multiple disciplines. By leveraging their diverse compositions, tunable properties, and ability to interact with guest molecules, researchers are paving the way for novel applications that could significantly impact areas such as healthcare, environmental science, and information technology.

Here are some examples of non-AIE$_{gen}$-based luminescent cages. Sun et al. have synthesized a novel POC named PyTC1, based on pyrene [54]. An exciting discovery was made regarding the interaction between cages, where a gentle C–H⋯π interaction caused an unforeseen change in the absorption behavior of the pyrene chromophore (Figure 3a). This alteration enabled using visible light for photocatalyzing the aerobic hydroxylation of benzeneboronic acid derivatives. By inducing an absorption shift through C–H⋯π interaction, the chromophore became capable of driving photocatalysis with visible light, surpassing its initial limitation to UV light activation. POCs derived from pyridine salt structures have a tendency to form supramolecular compounds that are soluble in water. A novel triangular prism-shaped hexagonal POC Cage-C was synthesized to overcome this limitation [55]. Cage-C displayed a larger cavity and flexible conformation, exhibiting strong fluorescence emission. Cage-C can undergo π-π interactions with polycyclic aromatic hydrocarbons like pyrene, leading to a gradual decrease in fluorescence intensity (Figure 3b). The fluorescence intensity continuously diminished by introducing pyrene to the Cage-C. By controlling the solubilities of Cage-C and pyrene, Cage-C could be recycled through phase separation in a mixed system comprising methanol, ether, and deionized water. By employing a metalloligand strategy, unreactive luminescent complexes resembling [Ru(bpy)3] have been incorporated into the linker segments of tetrahedral POCs [56]. These MOCs preserve the original complexes emission characteristics and exhibit remarkable stability, even at low concentrations, as they resist disassembly.

Martir et al. conducted research on the energy interaction and electron transfer in a photoactive cage 4PyCzBP-Pd consisting of encapsulated fluorescent dyes and a thermally activated delayed fluorescence (TADF) ligand [57]. The researchers introduced a simple method to activate the luminescent characteristics of a polyhedral assembly. This involved combining a TADF organic emitter with Pd^{2+} ions and a dipyridylcarbazole ligand structure, as illustrated in Figure 3c. This combination formed a luminescent Pd_6L_{12} molecular cube. A series of ligands and dipalladium(II) cages, modified with luminescent units, were synthesized [58]. Interestingly, both the ligands and cages demonstrated high insulation from the exo-functionalization. Their electronic transitions occurred in the UV light region, and the formation of the cage structure minimally influenced features of the excited state. Another study presented a group of self-assembled $Zn_8L_{12}X_4$ cages that incorporate organic fluorophores (R-sites such as naphthalenyl, pyrenyl, phenyl) and luminescence promotors (X-sites such as Cl, Br, I), as presented in Figure 3d [59]. These cages are connected through supramolecular interactions. The activation of effective radiative pathways, along with a decrease in nonradiative relaxations due to metal coordination, is achieved through the involvement of supramolecular interactions, particularly weak C−H⋯X interactions.
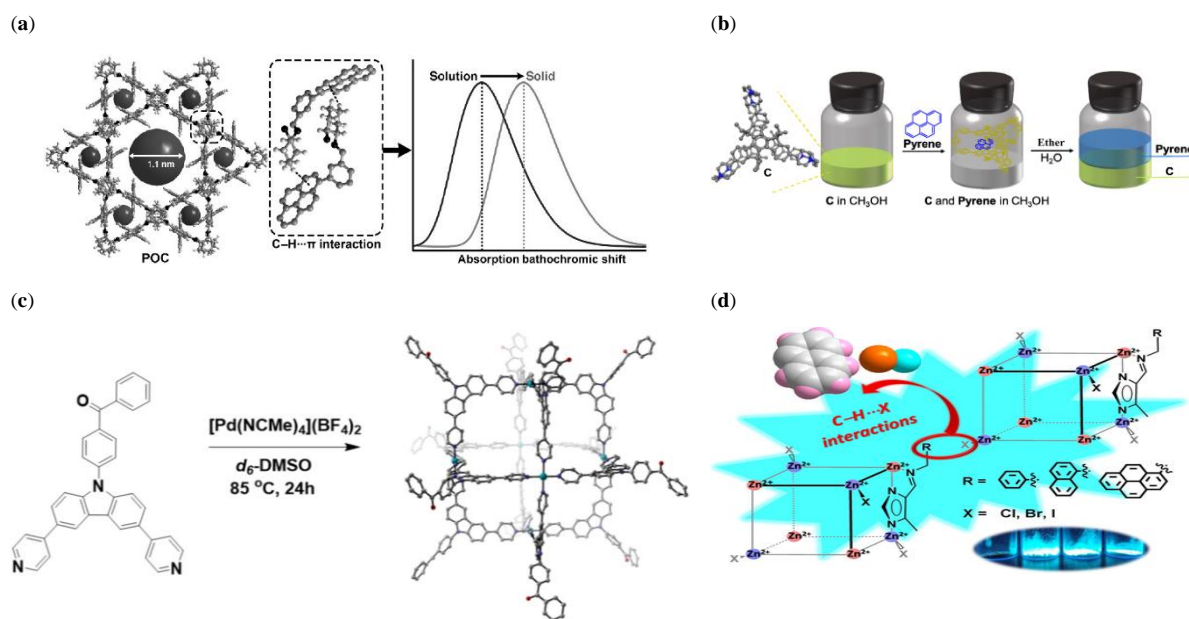
Figure 3. (**a**) Pyrene-based PyTC1 cage. Adapted with permission from ref. [54] Copyright © 2021 Chinese Chemical Society under an open access Creative Commons Attribution-NonCommercial 3.0 Unported license (CC BY-NC 3.0). (**b**) Interaction of Cage-C with pyrene and cage recycling. Adapted with permission from ref. [55] Copyright © 2023 MDPI under an open access Creative Common CC BY license. (**c**) Self-assembly between through Pd^{2+} ions to form the cage 4PyCzBP-Pd. Adapted with permission from ref. [57] Copyright © 2018 American Chemical Society. (**d**) The self-assembled $Zn_8L_{12}X_4$ cages. Adapted with permission from ref. [59] Copyright © 2018 Wiley-VCH Verlag GmbH & Co. KGaA, Weinheim, John Wiley and Sons.

4. CPL-Active Cages

This section focuses on discussing notable advancements in the field of CPL MOCs. MOCs, a fascinating category of self-assembled supramolecular materials, are constructed by coordinating metal ions with organic ligands. This bonding creates isolated structures instead of extended ones [18,33,60,61]. Two chiral coordination cages, Pd_6L_{12}, were synthesized using crown ether and methoxymethyl groups [31]. The cage, modified with crown ether groups, serves as a host by capturing anionic achiral dyes. This results in the formation of stable supramolecular complexes via metal coordination and interactions involving the host, guest, and cations. Encapsulating achiral dyes in hollow cages prevents ACQ and enhances the induction and amplification of CPL. The resulting dyes exhibit effective CPL, with high g_{lum} values and increased emission quantum yields in solution and the aggregated solid state (Figure 4a). The host-guest adducts crystallization further amplifies g_{lum} by one order of magnitude. As shown in Figure 4b, a post-assembly modification strategy was utilized to construct homochiral Ti_4L_6-based cages (Ti-b) with CPL response [34]. Combining a homochiral PTC-372 cage host with a chiral R-Camphorq guest enhances the temperature-dependent CPL, reaching 2.5×10^{-2} for g_{lum} values. These findings demonstrate the importance of these MOCs for CPL-based molecular recognition. A series of homochiral cubic MOCs were successfully synthesized [62]. These MOCs displayed robust circular dichroism (CD) signals and demonstrated comparable photoluminescence with similar quantum yields, attributed to the presence of different substituents. Using a chiral ancillary ligand induction strategy, Zhou et al. formed an enantiopure lanthanide tetrahedral cage. The resulting cage, $Eu_4L_4(L')_4$, exhibits strong CPL with g_{lum} values of 0.20 and ultrahigh emission quantum yields of up to 81%, Figure 4c [63]. Gu et al. employed a layer-by-layer growth strategy to synthesize crystalline chiral porous material films using racemic Ti_4L_6 cages (Ti-d) and homochiral metal complexes. The chiral signals in the films originated from the Ti_4L_6 cages, with g_{lum} values of about 0.002 for both (R, D)- and (S, K)-crystalline porous materials films (Figure 4d) [64].
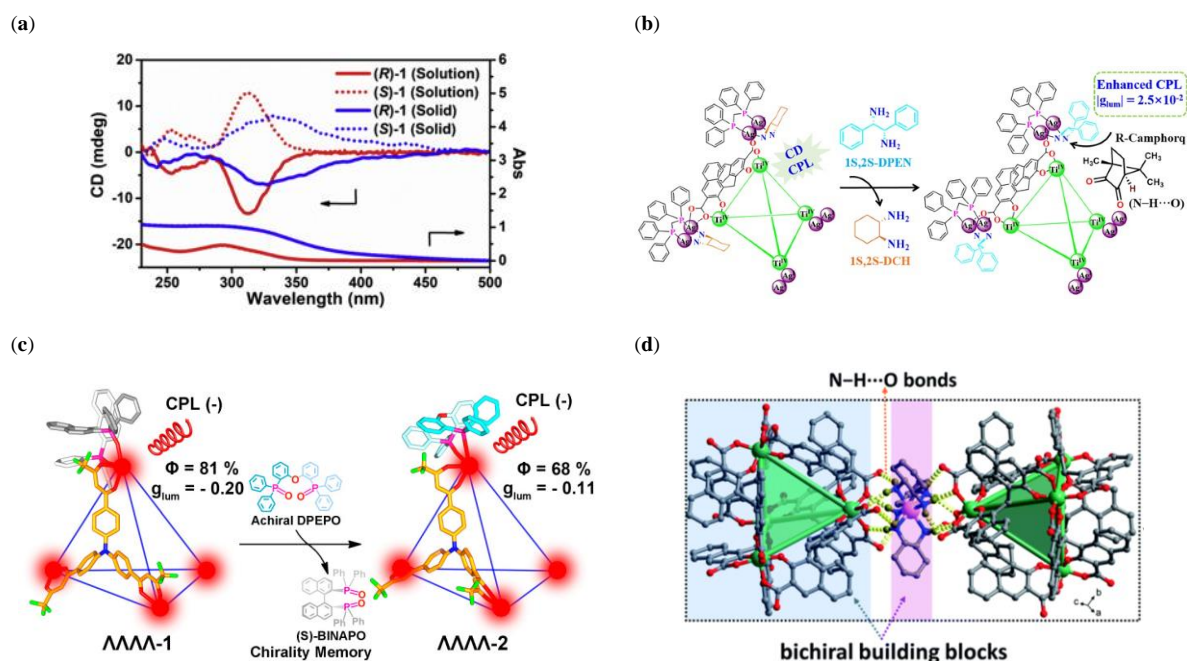
Figure 4. (**a**) The solution and solid-state CD and UV spectra of cage-dye adduct Pd_6L_{12}. Adapted with permission from ref. [31] Copyright © 2021 Elsevier Inc. (**b**) homochiral Ti_4L_6-based cages (Ti-b). Adapted with permission from ref. [34] Copyright © 2023 Science China Press. (**c**) A highly luminescent chiral tetrahedral $Eu_4L_4(L')_4$ Cage. Adapted with permission from ref. [63] Copyright © 2019 American Chemical Society. (**d**) Racemic Ti_4L_6 cages (Ti-d) and homochiral metal complexes. Adapted with permission from ref. [64] Copyright © 2021 The Royal Society of Chemistry under a Creative Commons Attribution-NonCommercial 3.0 Unported Licence.

Chiral coordination cages were prepared by coordinating helicene ligands with transition metals, resulting in Zn_2L_3 cages that demonstrated yellow CPL with a g_{lum} of 0.002. The Zn_2L_3 cages self-assembled into green-luminescent $Zn_6L_6(SO_4)_4$ cages with a twisted structure and chiral stacking upon adding Na_2SO_4, enhancing their CPL activity ($g_{lum} = 0.004$).[65] In 2020, a MOC called rac-MOC-52 was synthesized using a polypyridine Ru(II)-metalloligand. The resulting D-MOC-52 and K-MOC-52 exhibited glum values of about 0.004 at 703 nm, respectively. These findings position them as good candidates for circular polarization response and detection [66]. In 2021, stable cage-dye adducts were formed by integrating achiral dyes with the chiral Pd_6L_{12} cages. As a result of the aggregation and vibrational relaxation, these adducts exhibited amplified g_{lum} values (up to 0.024) in the crystalline state. Chirality was transferred to the dyes from the cage frameworks while efficiently inhibiting the ACQ effect. The resulting host-guest supramolecular complexes displayed high quantum yields (up to 34.8%) in both the solid state and concentrated solutions [31].

5. Applications of MOCs and POCs

Luminescent materials find applications in optoelectronics, sensing, electroluminescence, photocatalysis, and biomedicine. Luminescent porous materials based on AIE$_{gens}$ offer promising features such as reversible absorption, selective recognition, and recyclability. Challenges persist in sensing large metal ions in mesoporous hybrids. Recent progress includes luminescent POCs and MOCs for detecting metal ions, biomolecules, vapors, gases, and explosives. This discussion will discuss representative examples highlighting some applications, such as sensing and enantioselectivity.

5.1. Sensing

Luminescence is a widely used technique in sensing applications. AIE$_{gens}$ emission 'turn-on' behavior enables their application in sensing. Combining AIE$_{gens}$ with metallacages preserves their desirable photophysical traits and may introduce novel responsiveness through interactions with building blocks [47,67,68]. The design and luminescent characteristics of platinum(II) tetragonal prismatic cages composed of multiple components were reported [51]. Specifically, Cage-44 (Figure 5a) was utilized as a fluorescent sensor that undergoes a self-destructive reaction in the presence of amino acids, but it can be restored by introducing Pt(II) acceptors. These investigations contribute to the advancement of fluorescent materials research and provide a pathway for

developing supramolecular coordination complexes that respond to stimuli. A unique trefoil-shaped MOC-11 (Figure 5b) assembles into a porous three-dimensional supramolecular structure via C–H···O interactions [69]. MOC-11 exhibited high sensitivity and selectivity to detect Fe^{3+}, $Cr_2O_7^{2-}$, nitrofuran antibiotics, and nitroimidazole antibiotics in aqueous solutions. The cage Zr-MOC was utilized as a fluorescent probe for phosphate detection in water samples, Figure 5c [70]. This probe exhibited several advantages, including good selectivity and linearity and a low detection limit, making it suitable for practical sample detection. At low concentrations, phosphate particularly binds to the Zr site, obstructing the LMCT effect and causing the aggregation of multiple cages, resulting in enhanced fluorescence. When present at higher concentrations, phosphate displaces the ligands within the cages, resulting in the formation of an amorphous derivative. This derivative was thoroughly examined and evaluated for its possible uses in catalysis and adsorption. A water-soluble fluorescent POC called RCC19R showed great sensitivity and selectivity for detecting Au^{3+} in aqueous solutions, Figure 5d.[71]. RCC19R was employed as a fluorescent probe with ratiometric properties, allowing for the quantitative detection of Au^{3+} ions released from the gold nanoparticles dissociation. Remarkably, this sensing method demonstrated excellent accuracy, selectivity, and sensitivity in biological fluids and environmental water. The findings highlight the significant potential of the water-soluble cage for fluorescence sensing applications.
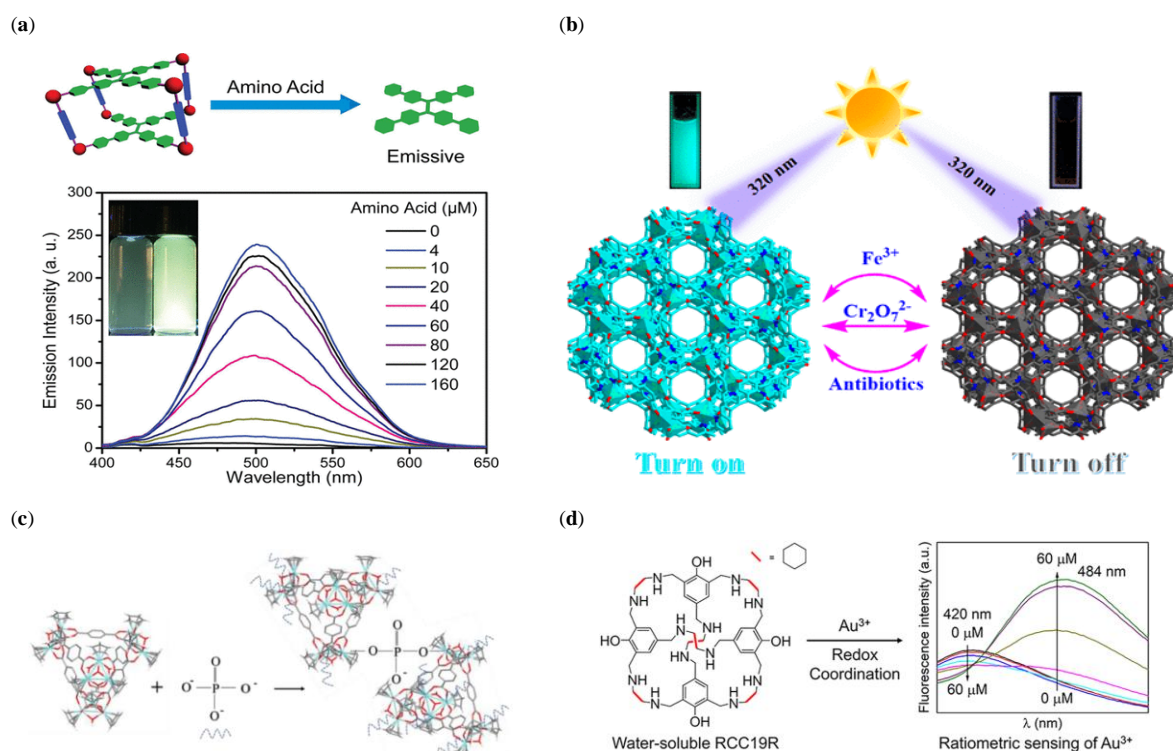

Figure 5. (**a**) Amino acid sensing of Cage-44. Adapted with permission from ref. [51] Copyright © 2017 American Chemical Society. (**b**) Cage MOC-11 as fluorescent chemosensor. Adapted with permission from ref. [69] Copyright © 2023, American Chemical Society. (**c**) Schematic illustrates the agglomeration of Zr-MOC triggered by phosphate. Adapted with permission from ref. [70] Copyright © 2022 Published by Elsevier B.V. on behalf of Chinese Chemical Society and Institute of Materia Medica, Chinese Academy of Medical Sciences. (**d**) Cage RCC19R is used to quantitatively detect Au^{3+} ions released from the dissociation of gold nanoparticles. Adapted with permission from ref. [71] Copyright © 2021 Elsevier B.V.

5.2. Enantioselectivity

Organic cages find valuable applications in enantioselective processes, demonstrating impressive selectivity by incorporating chiral components. They have been utilized in enantioselective catalysis, chiral separation, and molecular recognition, offering tailored receptors for specific enantiomers. These versatile structures enable efficient and sustainable development of asymmetric methodologies in various industries. In the following examples, we will showcase the application of organic cages in enantioselective processes. A pair of multi-functional cages, namely 3P-1 and 3M-1, which possess chirality, luminescence, and porosity, were successfully synthesized [72]. The synthesis process was efficient, resulting in high yields, and purification was easily achieved through precipitation without the need for column chromatography separation. Due to the combined effects of

chirality and porosity in the solid state, both cages exhibited excellent enantioselectivity in adsorbing various aromatic racemates. That research presents a valuable approach to constructing multi-functional chiral cages with potential molecular recognition and chiral separation applications. In 2021, a new approach was introduced to selectively determine the enantiomers of amino acids and hydroxy acids using a fluorescent organic cage called CC3-R as a sensor [73]. CC3-R displayed distinct fluorescence responses, with D/L-tyrosine leading to fluorescence enhancement and R/S-mandelic acid causing fluorescence quenching. That study demonstrated the prospective application of organic cages in enantioselective analysis based on fluorescence and highlighted the influence of solvent on fluorescence signals. Moreover, the expanding range of chiral organic cages offers opportunities for chiral recognition using alternative analytical techniques. By carefully selecting an appropriate organic cage, the fluorescence-based recognition of particular enantiomers can be achieved by controlling the fluorescence intensity. In the year 2023, researchers successfully created C3-symmetric POCs to achieve effective enantioseparation [74]. These materials displayed significant enantioselectivity, indicating their usefulness in chiral separation and purification processes. Recent studies have highlighted how restricting conformational flexibility and incorporating hydrogen bonding functional groups in ligands can affect the chiral self-sorting and hierarchical self-assembly of metal-organic cages [75]. In recent years, technologies for chiral recognition and resolution have found extensive applications in pharmaceuticals, materials science, and food industries. For instance, in pharmaceuticals, these technologies can be used to produce optically pure drugs, enhance drug efficacy, and minimize adverse reactions [76]. Additionally, chiral metal-organic cage-modified polyvinylidene fluoride membranes have been developed through metal phenolic networks for the purpose of enantioseparation [77].

6. Conclusion and Future Perspectives

This review highlights recent advancements in luminescent cages, focusing on AIE_{gen}-based, CPL-active, and non-AIEgen cages, along with their applications in sensing and enantioselectivity. The well-defined structures of these cages facilitate effective use of their photophysical properties. AIE_{gen}-based crystalline cages, such as POCs and MOCs, show significant luminescence by limiting intramolecular motion, while AIE-active metallacages present promising applications in biomedicine, solid-state lighting, chemosensing, and gas storage. The review underscores the need to explore future prospects, including the development of stable AIE-based POCs and MOCs for practical uses. Understanding molecular influences on light absorption and topology's role in functionality is crucial. While TPE-based sensors are prevalent, TPE-free frameworks could reveal new insights. Current research primarily involves lanthanides and noble metals, with computational methods expected to aid in predicting self-assembly and interactions. Future efforts in CPL organic cages should focus on enhancing luminescence efficiency, chiral sensing, hybrid system integration, and applications in bioimaging and optoelectronics. These advancements could lead to innovative technologies and smart materials. Ultimately, the review aims to inspire researchers to develop novel luminous organic cages with diverse applications.

Author Contributions: O.Y.: Conceptualization, Validation, Visualization, Writing—original draft, Writing—review & editing. X.X.: Conceptualization, Validation. J.Y.: Validation, Visualization. K.I.A.: Conceptualization, Validation. E.A.B.: Conceptualization, Validation. X.Y.: Conceptualization, Supervision, Funding acquisition, Validation, Project administration, Writing—review & editing. All authors have read and agreed to the published version of the manuscript.

Institutional Review Board Statement: Not applicable

Informed Consent Statement: Not applicable

Data Availability Statement: The data provided in this study can be found within the article.

Conflicts of Interest: The authors declare that they have no competing interests.

References

1. Yang, Z.; Cao, J.; He, Y.; Yang, J.H.; Kim, T.; Peng, X.; Kim, J.S. Macro-/micro-environment-sensitive chemosensing and biological imaging. *Chem. Soc. Rev.* **2014**, *43*, 4563–4601.
2. Stender, A.S.; Marchuk, K.; Liu, C.; Sander, S.; Meyer, M.W.; Smith, E.A.; Neupane, B.; Wang, G.; Li, J.; Cheng, J.-X.; et al. Single Cell Optical Imaging and Spectroscopy. *Chem. Rev.* **2013**, *113*, 2469–2527.

3. Yang, S.K.; Shi, X.; Park, S.; Ha, T.; Zimmerman, S.C. A dendritic single-molecule fluorescent probe that is monovalent, photostable and minimally blinking. *Nat. Chem.* **2013**, *5*, 692–697.

4. Zhu, M.; Yang, C. Blue fluorescent emitters: Design tactics and applications in organic light-emitting diodes. *Chem. Soc. Rev.* **2013**, *42*, 4963–4976.

5. Maggini, L.; Bonifazi, D. Hierarchised luminescent organic architectures: Design, synthesis, self-assembly, self-organisation and functions. *Chem. Soc. Rev.* **2012**, *41*, 211–241.

6. Ma, L.; Feng, X.; Wang, S.; Wang, B. Recent advances in AIEgen-based luminescent metal–organic frameworks and covalent organic frameworks. *Mater. Chem. Front.* **2017**, *1*, 2474–2486.

7. Herwig, L.; Rice, A.J.; Bedbrook, C.N.; Zhang, R.K.; Lignell, A.; Cahn, J.K.B.; Renata, H.; Dodani, S.C.; Cho, I.; Cai, L.; et al. Directed Evolution of a Bright Near-Infrared Fluorescent Rhodopsin Using a Synthetic Chromophore. *Cell Chem. Biol.* **2017**, *24*, 415–425.

8. Mei, J.; Leung, N.L.C.; Kwok, R.T.K.; Lam, J.W.Y.; Tang, B.Z. Aggregation-Induced Emission: Together We Shine, United We Soar! *Chem. Rev.* **2015**, *115*, 11718–11940.

9. Aly, K.I.; Younis, O.; Mahross, M.H.; Orabi, E.A.; Abdel-Hakim, M.; Tsutsumi, O.; Mohamed, M.G.; Sayed, M.M. Conducting copolymers nanocomposite coatings with aggregation-controlled luminescence and efficient corrosion inhibition properties. *Progress. Org. Coat.* **2019**, *135*, 525–535.

10. Sayed, M.; Younis, O.; Hassanien, R.; Ahmed, M.; Mohammed, A.A.K.; Kamal, A.M.; Tsutsumi, O. Design and Synthesis of Novel Indole Derivatives with Aggregation-Induced Emission and Antimicrobial Activity. *J. Photochem. Photobiol. A: Chem.* **2019**, *383*, 111969–111979.

11. Younis, O.; Orabi, E.A.; Kamal, A.M.; Sayed, M.; Hassanien, R.; Davis, R.L.; Tsutsumi, O.; Ahmed, M. Aggregation-induced emission with white, green, or blue luminescence from biologically-active indole derivatives. *Opt. Mater.* **2020**, *100*, 109713.

12. Younis, O.; Tolba, M.S.; Orabi, E.A.; Kamal, A.M.; Hassanien, R.; Tsutsumi, O.; Ahmed, M. Biologically-Active Heterocyclic Molecules with Aggregation-Induced Blue-Shifted Emission and Efficient Luminescence both in Solution and Solid States. *J. Photochem. Photobiol. A Chem.* **2020**, *400*, 112642.

13. Hong, Y.; Lam, J.W.Y.; Tang, B.Z. Aggregation-induced emission. *Chem. Soc. Rev.* **2011**, *40*, 5361–5388.

14. Hong, Y.; Lam, J.W.Y.; Tang, B.Z. Aggregation-induced emission: Phenomenon, mechanism and applications. *Chem. Commun.* **2009**, 4332–4353. https://doi.org/10.1039/B904665H(2009).

15. Asad, M.; Anwar, M.I.; Abbas, A.; Younas, A.; Hussain, S.; Gao, R.; Li, L.-K.; Shahid, M.; Khan, S. AIE based luminescent porous materials as cutting-edge tool for environmental monitoring: State of the art advances and perspectives. *Coord. Chem. Rev.* **2022**, *463*, 214539.

16. Castilla, A.M.; Ramsay, W.J.; Nitschke, J.R. Stereochemistry in Subcomponent Self-Assembly. *Acc. Chem. Res.* **2014**, *47*, 2063–2073.

17. Custelcean, R. Anion encapsulation and dynamics in self-assembled coordination cages. *Chem. Soc. Rev.* **2014**, *43*, 1813–1824.

18. Amouri, H.; Desmarets, C.; Moussa, J. Confined Nanospaces in Metallocages: Guest Molecules, Weakly Encapsulated Anions, and Catalyst Sequestration. *Chem. Rev.* **2012**, *112*, 2015–2041.

19. Yoshizawa, M.; Tamura, M.; Fujita, M. Diels-Alder in Aqueous Molecular Hosts: Unusual Regioselectivity and Efficient Catalysis. *Science* **2006**, *312*, 251–254.

20. Zhu, C.-Y.; Pan, M.; Su, C.-Y. Metal-Organic Cages for Biomedical Applications. *Isr. J. Chem.* **2019**, *59*, 209–219.

21. Lustig, W.P.; Mukherjee, S.; Rudd, N.D.; Desai, A.V.; Li, J.; Ghosh, S.K. Metal–organic frameworks: Functional luminescent and photonic materials for sensing applications. *Chem. Soc. Rev.* **2017**, *46*, 3242–3285.

22. Hu, Z.; Deibert, B.J.; Li, J. Luminescent metal–organic frameworks for chemical sensing and explosive detection. *Chem. Soc. Rev.* **2014**, *43*, 5815–5840.

23. Longhi, G.; Castiglioni, E.; Koshoubu, J.; Mazzeo, G.; Abbate, S. Circularly Polarized Luminescence: A Review of Experimental and Theoretical Aspects. *Chirality* **2016**, *28*, 696–707.

24. Ikeda, T.; Masuda, T.; Hirao, T.; Yuasa, J.; Tsumatori, H.; Kawai, T.; Haino, T. Circular dichroism and circularly polarized luminescence triggered by self-assembly of tris(phenylisoxazolyl)benzenes possessing a perylenebisimide moiety. *Chem. Commun.* **2012**, *48*, 6025–6027.

25. Carr, R.; Evans, N.H.; Parker, D. Lanthanide complexes as chiral probes exploiting circularly polarized luminescence. *Chem. Soc. Rev.* **2012**, *41*, 7673–7686.

26. Xu, Y.; Yang, G.; Xia, H.; Zou, G.; Zhang, Q.; Gao, J. Enantioselective synthesis of helical polydiacetylene by application of linearly polarized light and magnetic field. *Nat. Commun.* **2014**, *5*, 5050.

27. Kim, J.; Lee, J.; Kim, W.Y.; Kim, H.; Lee, S.; Lee, H.C.; Lee, Y.S.; Seo, M.; Kim, S.Y. Induction and control of supramolecular chirality by light in self-assembled helical nanostructures. *Nat. Commun.* **2015**, *6*, 6959.

28. David, A.H.G.; Casares, R.; Cuerva, J.M.; Campaña, A.G.; Blanco, V. A [2]Rotaxane-Based Circularly Polarized Luminescence Switch. *J. Am. Chem. Soc.* **2019**, *141*, 18064–18074.

29. Tanaka, H.; Inoue, Y.; Mori, T. Circularly Polarized Luminescence and Circular Dichroisms in Small Organic Molecules: Correlation between Excitation and Emission Dissymmetry Factors. *ChemPhotoChem* **2018**, *2*, 386–402.

30. He, C.; Yang, G.; Kuai, Y.; Shan, S.; Yang, L.; Hu, J.; Zhang, D.; Zhang, Q.; Zou, G. Dissymmetry enhancement in enantioselective synthesis of helical polydiacetylene by application of superchiral light. *Nat. Commun.* **2018**, *9*, 5117.

31. Tang, X.; Jiang, H.; Si, Y.; Rampal, N.; Gong, W.; Cheng, C.; Kang, X.; Fairen-Jimenez, D.; Cui, Y.; Liu, Y. Endohedral functionalization of chiral metal-organic cages for encapsulating achiral dyes to induce circularly polarized luminescence. *Chem* **2021**, *7*, 2771–2786.

32. Li, R.-J.; Holstein, J.J.; Hiller, W.G.; Andréasson, J.; Clever, G.H. Mechanistic Interplay between Light Switching and Guest Binding in Photochromic [Pd2Dithienylethene4] Coordination Cages. *J. Am. Chem. Soc.* **2019**, *141*, 2097–2103.

33. Luo, X.-Y.; Pan, M. Metal-organic materials with circularly polarized luminescence. *Coord. Chem. Rev.* **2022**, *468*, 214640.

34. Chen, G.-H.; He, Y.-P.; Yu, Y.; Li, Q.-H.; Zhang, J. Homochiral design of titanium-organic cage for circularly polarized luminescence-based molecular detection. *Sci. China Chem.* **2023**, *66*, 2558–2562.

35. Yu, S.; Yan, W.; Long, W.; Yuan, Y.; Ouyang, H.; He, Z.; Tian, J.; Liu, M.; Zhang, X.; Wei, Y. A facile strategy to fabricate fluorescent polymeric nanoparticles with aggregation-induced emission feature via oxygen-tolerated light-induced living polymerization. *Dye. Pigment.* **2021**, *192*, 109454.

36. Chen, G.-H.; He, Y.-P.; Yu, Y.; Lv, H.; Li, S.; Wang, F.; Gu, Z.-G.; Zhang, J. Post-Assembly Modification of Homochiral Titanium–Organic Cages for Recognition and Separation of Molecular Isomers. *Angew. Chem. Int. Ed.* **2023**, *62*, e202300726.

37. McTernan, C.T.; Ronson, T.K.; Nitschke, J.R. Post-assembly Modification of Phosphine Cages Controls Host–Guest Behavior. *J. Am. Chem. Soc.* **2019**, *141*, 6837–6842.

38. Briggs, M.E.; Cooper, A.I. A Perspective on the Synthesis, Purification, and Characterization of Porous Organic Cages. *Chem. Mater.* **2017**, *29*, 149–157.

39. Pilgrim, B.S.; Champness, N.R. Metal-Organic Frameworks and Metal-Organic Cages—A Perspective. *Chempluschem* **2020**, *85*, 1842–1856.

40. Zhu, Q.; Qu, H.; Avci, G.; Hafizi, R.; Zhao, C.; Day, G.M.; Jelfs, K.E.; Little, M.A.; Cooper, A.I. Computationally guided synthesis of a hierarchical [4[2+3]+6] porous organic 'cage of cages'. *Nat. Synth.* **2024**, *3*, 825–834.

41. Jia, L.; Tang, X.; Cui, Y.; Liu, Y. Porous metal-organic cage-based membranes. *Sci. China Chem.* **2023**, *66*, 2169–2180.

42. Qin, Y.; Ling, Q.-H.; Wang, Y.-T.; Hu, Y.-X.; Hu, L.; Zhao, X.; Wang, D.; Yang, H.-B.; Xu, L.; Tang, B.Z. Construction of Covalent Organic Cages with Aggregation-Induced Emission Characteristics from Metallacages for Mimicking Light-Harvesting Antenna. *Angew. Chem. Int. Ed.* **2023**, *62*, e202308210.

43. Zhang, X.; Shi, J.; Shen, G.; Gou, F.; Cheng, J.; Zhou, X.; Xiang, H. Non-conjugated fluorescent molecular cages of salicylaldehyde-based tri-Schiff bases: AIE, enantiomers, mechanochromism, anion hosts/probes, and cell imaging properties. *Mater. Chem. Front.* **2017**, *1*, 1041–1050.

44. Sun, Y.-L.; Wang, Z.; Ren, C.; Zhang, J.; Zhang, H.; Zhang, C.; Tang, B.Z. Highly Emissive Organic Cage in Single-Molecule and Aggregate States by Anchoring Multiple Aggregation-Caused Quenching Dyes. *ACS Appl. Mater. Interfaces* **2022**, *14*, 53567–53574.

45. Zou, D.; Li, Z.; Long, D.; Dong, X.; Qu, H.; Yang, L.; Cao, X. Molecular Cage with Dual Outputs of Photochromism and Luminescence Both in Solution and the Solid State. *ACS Appl. Mater. Interfaces* **2023**, *15*, 13545–13553.

46. Zhao, J.; Zhou, Z.; Li, G.; Stang, P.J.; Yan, X. Light-emitting self-assembled metallacages. *Natl. Sci. Rev.* **2021**, *8*, nwab045.

47. Yan, X.; Cook, T.R.; Wang, P.; Huang, F.; Stang, P.J. Highly emissive platinum(II) metallacages. *Nat. Chem.* **2015**, *7*, 342–348.

48. Yan, X.; Wang, M.; Cook, T.R.; Zhang, M.; Saha, M.L.; Zhou, Z.; Li, X.; Huang, F.; Stang, P.J. Light-Emitting Superstructures with Anion Effect: Coordination-Driven Self-Assembly of Pure Tetraphenylethylene Metallacycles and Metallacages. *J. Am. Chem. Soc.* **2016**, *138*, 4580–4588.

49. XYan; Wei, P.; Liu, Y.; Wang, M.; Chen, C.; Zhao, J.; Li, G.; Saha, M.L.; Zhou, Z.; An, Z.; Li, X.; et al. Endo- and Exo-Functionalized Tetraphenylethylene M12L24 Nanospheres: Fluorescence Emission inside a Confined Space. *J. Am. Chem. Soc.* **2019**, *141*, 9673–9679.

50. Li, H.; Xie, T.-Z.; Liang, Z.; Dahal, D.; Shen, Y.; Sun, X.; Yang, Y.; Pang, Y.; Liu, T. Conformational change due to intramolecular hydrophobic interaction leads to large blue-shifted emission from single molecular cage solutions. *Chem. Commun.* **2019**, *55*, 330–333.

51. Zhang, M.; Saha, M.L.; Wang, M.; Zhou, Z.; Song, B.; Lu, C.; Yan, X.; Li, X.; Huang, F.; Yin, S.; et al. Multicomponent Platinum(II) Cages with Tunable Emission and Amino Acid Sensing. *J. Am. Chem. Soc.* **2017**, *139*, 5067–5074.

52. Zhou, Z.; Yan, X.; Saha, M.L.; Zhang, M.; Wang, M.; Li, X.; Stang, P.J. Immobilizing Tetraphenylethylene into Fused Metallacyles: Shape Effects on Fluorescence Emission. *J. Am. Chem. Soc.* **2016**, *138*, 13131–13134.

53. Li, M.; Jiang, S.; Zhang, Z.; Hao, X.-Q.; Jiang, X.; Yu, H.; Wang, P.; Xu, B.; Wang, M.; Tian, W. Tetraphenylethylene-Based Emissive Supramolecular Metallacages Assembled by Terpyridine Ligands. *CCS Chem.* **2020**, *2*, 337–348.

54. Sun, N.; Qi, D.; Jin, Y.; Wang, H.; Wang, C.; Qu, C.; Liu, J.; Jin, Y.; Zhang, W.; Jiang, J. Porous Pyrene Organic Cage with Unusual Absorption Bathochromic-Shift Enables Visible Light Photocatalysis. *CCS Chem.* **2021**, *4*, 2588–2596.

55. Song, H.; Guo, Y.; Zhang, G.; Shi, L. Tailored Water-Soluble Covalent Organic Cages for Encapsulation of Pyrene and Information Encryption. International Journal of Molecular Sciences, 2023.

56. Luis, E.T.; Iranmanesh, H.; Arachchige, K.S.A.; Donald, W.A.; Quach, G.; Moore, E.G.; Beves, J.E. Luminescent Tetrahedral Molecular Cages Containing Ruthenium(II) Chromophores. *Inorg. Chem.* **2018**, *57*, 8476–8486.

57. Martir, D.R.; Pizzolante, A.; Escudero, D.; Jacquemin, D.; Warriner, S.L.; Zysman-Colman, E. Photoinduced Energy and Electron Transfer Between a Photoactive Cage Based on a Thermally Activate Delayed Fluorescence Ligand and Encapsulated Fluorescent Dyes. *ACS Appl. Energy Mater.* **2018**, *1*, 2971–2978.

58. Elliott, A.B.S.; Lewis, J.E.M.; van der Salm, H.; McAdam, C.J.; Crowley, J.D.; Gordon, K.C. Luminescent Cages: Pendant Emissive Units on [Pd2L4]4+ "Click" Cages. *Inorg. Chem.* **2016**, *55*, 3440–3447.

59. Luo, D.; Li, M.; Zhou, X.-P.; Li, D. Boosting Luminescence of Planar-Fluorophore-Tagged Metal–Organic Cages Via Weak Supramolecular Interactions. *Chem. A Eur. J.* **2018**, *24*, 7108–7113.

60. El-Sayed, E.-S.M.; Yuan, D. Metal-Organic Cages (MOCs): From Discrete to Cage-based Extended Architectures. *Chem. Lett.* **2020**, *49*, 28–53.

61. Zarra, S.; Wood, D.M.; Roberts, D.A.; Nitschke, J.R. Molecular containers in complex chemical systems. *Chem. Soc. Rev.* **2015**, *44*, 419–432.

62. Wang, X.-Z.; Sun, M.-Y.; Huang, Z.; Xie, M.; Huang, R.; Lu, H.; Zhao, Z.; Zhou, X.-P.; Li, D. Turn-On Circularly Polarized Luminescence in Metal–Organic Frameworks. *Adv. Opt. Mater.* **2021**, *9*, 2002096.

63. Zhou, Y.; Li, H.; Zhu, T.; Gao, T.; Yan, P. A Highly Luminescent Chiral Tetrahedral Eu4L4(L′)4 Cage: Chirality Induction, Chirality Memory, and Circularly Polarized Luminescence. *J. Am. Chem. Soc.* **2019**, *141*, 19634–19643.

64. Chen, H.; Gu, Z.-G.; Zhang, J. Surface chiroselective assembly of enantiopure crystalline porous films containing bichiral building blocks. *Chem. Sci.* **2021**, *12*, 12346–12352.

65. Ding, Y.; Shen, C.; Gan, F.; Wang, J.; Zhang, G.; Li, L.; Shu, M.; Zhu, B.; Crassous, J.; Qiu, H. Tunable construction of transition metal-coordinated helicene cages. *Chin. Chem. Lett.* **2021**, *32*, 3988–3992.

66. Li, C.; Liu, Y.; Wang, Y.; Guo, J.; Pan, M. Assembly and properties of Pd4Ru8 metal-organic cages based on polypyridine Ru (II)-metalloligand. Sci. *Sin. Chim.* **2020**, *50*, 687–694.

67. Zhang, Z.; Zhao, Z.; Wu, L.; Lu, S.; Ling, S.; Li, G.; Xu, L.; Ma, L.; Hou, Y.; Wang, X.; et al. Emissive Platinum(II) Cages with Reverse Fluorescence Resonance Energy Transfer for Multiple Sensing. *J. Am. Chem. Soc.* **2020**, *142*, 2592–2600.

68. Li, C.; Zhang, B.; Dong, Y.; Li, Y.; Wang, P.; Yu, Y.; Cheng, L.; Cao, L. A tetraphenylethene-based Pd2L4 metallacage with aggregation-induced emission and stimuli-responsive behavior. *Dalton Trans.* **2020**, *49*, 8051–8055.

69. Meng, Z.; Yang, F.; Wang, X.; Shan, W.-L.; Liu, D.; Zhang, L.; Yuan, G. Trefoil-Shaped Metal–Organic Cages as Fluorescent Chemosensors for Multiple Detection of Fe^{3+}, $Cr_2O_7^{2-}$, and Antibiotics. *Inorg. Chem.* **2023**, *62*, 1297–1305.

70. Gao, Z.; Jia, J.; Fan, W.; Liao, T.; Zhang, X. Zirconium metal organic cages: From phosphate selective sensing to derivate forming. *Chin. Chem. Lett.* **2022**, *33*, 4415–4420.

71. Dai, C.; Gu, B.; Tang, S.-P.; Deng, P.-H.; Liu, B. Fluorescent porous organic cage with good water solubility for ratiometric sensing of gold(III) ion in aqueous solution. *Anal. Chim. Acta* **2022**, *1192*, 339376.

72. Sun, Y.-L.; Wang, Z.; Ma, H.; Zhang, Q.-P.; Yang, B.-B.; Meng, X.; Zhang, Y.; Zhang, C. Chiral emissive porous organic cages. *Chem. Commun.* **2023**, *59*, 302–305.

73. Liu, Y.; Jia, J.; Liao, T.; Luo, J.; Zhang, X. Porous organic cage for enantiomeric fluorescence recognition of amino acid and hydroxy acid. *Luminescence* **2021**, *36*, 2022–2027.

74. Li, T.; Pan, Y.; Song, H.; Jiang, H.; Guo, Y.; Shi, L.; Hao, X.; Song, M.-P. Luminescent covalent organic cages with a C3-symmetric structure for effective enantioseparation. *New J. Chem.* **2023**, *47*, 22320–22325.

75. Ghorai, S.; Natarajan, R. Chiral Self-Sorting, Spontaneous Resolution, and Hierarchical Self-Assembly in Metal–Organic Cages. *Small* **2024**, *20*, 2400842.

76. Li, T.; Pan, Y.; Ding, L.; Kang, Y.; Hao, X.-Q.; Guo, Y.; Shi, L. Chiral cage materials with tailored functionalities for enantioselective recognition and separation. *Chem. Synth.* **2024**, *4*, 35.

77. Liu, C.; Li, J.; Lu, M.; Jia, X.; Yu, A.; Zhang, S. Chiral metal-organic cage modified polyvinylidene fluoride membrane via metal phenolic networks for enantioseparation. *Sep. Purif. Technol.* **2024**, *332*, 125765.